



Review

Doping of high concentration of Beryllium in GaAs layers, by molecular-beam epitaxy

J.P. Noh^a, G.B. Cho^a, D.W. Jung^b, N. Otsuka^b, T.H. Nam^a, K.W. Kim^{a,*}^a PRC for Nano-Morphic Biological Energy Conversion and Storage, Gyeongsang National University, 900 Gazwa-dong, Jinju 600-701, South Korea^b School of Materials Science, Japan Advanced Institute of Science and Technology, Asahidai 1-1, Nomishi, Ishikawa 923-1292, Japan

ARTICLE INFO

Article history:

Received 30 June 2009

Received in revised form 30 April 2010

Accepted 30 April 2010

Available online 6 May 2010

Keywords:

Low-temperature MBE growth

Non-equilibrium structure

Long-distance diffusion

ABSTRACT

Doping processes of high concentrations of Be in GaAs layers by molecular-beam epitaxy (MBE) at low temperatures with different growth rates were investigated in order to explore the possibility of the low-temperature MBE growth for obtaining highly non-equilibrium structures. A high concentration of acceptor Be atoms with a hole concentration of $5.65 \times 10^{20} \text{ cm}^{-3}$ were obtained with a substrate temperature 300°C and a low growth rate $0.03 \mu\text{m/h}$, while an increase in either the substrate temperature or the growth rate resulted in lower hole concentrations. These results suggest unique properties of the low-temperature MBE growth; long-distance diffusions of solute atoms are inhibited at a low growth temperature, while a low growth rate gives surface or near-surface atoms a sufficient time to form a low-energy configuration at a low growth temperature.

© 2010 Elsevier B.V. All rights reserved.

Contents

1. Introduction	71
2. Experimental	72
3. Results and discussion	72
4. Conclusions	75
Acknowledgment	75
References	75

1. Introduction

In the past two decades molecular-beam epitaxy (MBE) growth at low temperatures has been utilized for the development of novel semiconductor materials such as low-temperature grown GaAs (LT-GaAs) layers [1] and $\text{Ga}_{1-x}\text{Mn}_x\text{As}$ diluted magnetic semiconductors [2]. By the MBE growth at low temperatures highly super-saturated semiconductor alloys with high crystalline qualities can be obtained. In the case of LT-GaAs layers, significantly non-stoichiometric crystals are obtained, resulting in ultra-short life times of photo-excited carriers [1]. Concentrations of excess As atoms in LT-GaAs layers are far higher than those in crystals grown under the nearly equilibrium condition. In the case of $\text{Ga}_{1-x}\text{Mn}_x\text{As}$, a high concentration of substitutional Mn atoms is incorporated by the low-temperature growth, which leads to the ferromagnetism of this material. If a crystal is grown at a temperature normally

used for the growth of GaAs, MnAs crystals form inside the grown layer as the second phase. Theoretical study [3] indicates that a higher Curie temperature of $\text{Ga}_{1-x}\text{Mn}_x\text{As}$ can be obtained with a higher substitutional Mn concentration and a higher hole concentration. In recent studies [4–6], a great deal efforts have been made in order to increase the substitutional Mn concentration by the low-temperature MBE growth, but Curie temperatures obtained in these studies are still considerably lower than room temperature.

Microscopic processes of the low-temperature MBE growth of GaAs layers were extensively studied in the past [7,8]. In view of the afore-mentioned recent studies on $\text{Ga}_{1-x}\text{Mn}_x\text{As}$, however, further investigations are necessary in order to accurately understand the role of the low-temperature MBE growth in obtaining highly super-saturated semiconductor structures. In this paper we present results of a study on the doping processes of Be in the low-temperature MBE growth of GaAs layer. Beryllium is commonly used for the MBE growth of GaAs as acceptor impurity [9]. The doping processes have been widely investigated for a variety of growth conditions. Doping of this impurity at low temperatures, therefore, can be used for investigation of the role of the low-temperature

* Corresponding author. Tel.: +82 55 751 5305; fax: +82 55 751 6539.
E-mail address: kiwonkim@gnu.ac.kr (K.W. Kim).

Table 1
Growth conditions, carrier concentrations and change of (004) interplaner spacing $\Delta d/d$ of six samples.

No.	g ($\mu\text{m}/\text{h}$)	T_{Be} ($^{\circ}\text{C}$)	T_{S} ($^{\circ}\text{C}$)	t (μm)	R_{s} (Ω)	ρ (cm^{-3})	$\Delta d/d$
A	0.1	950	300	0.1	94.92	1.47×10^{20}	-1.03×10^{-3}
B	0.03	880	300	0.1	37.6	5.65×10^{20}	-2.47×10^{-3}
C	1	1030	300	0.3	38.5	3.65×10^{20}	-2.35×10^{-3}
D	0.1	1030	300	0.1	137.3	1.02×10^{20}	–
E	0.03	950	250	0.1	71.45	3.22×10^{20}	-3.60×10^{-3}
F	0.03	1000	250	0.1	65.69	3.47×10^{20}	-8.90×10^{-3}

MBE growth in producing highly super-saturated semiconductor structures. According to earlier studies [10–14], Be atoms tend to occupy interstitial sites and diffuse towards the surface or the substrate when a high concentration of Be atoms were doped. In the present study, we investigated how the concentrations of acceptor Be changed with the growth temperature and the growth rate in order to clarify the microscopic processes which determined their maximum concentrations in the low-temperature growth.

2. Experimental

Beryllium-doped GaAs layers were grown by utilizing a conventional MBE system. Semi-insulating epitaxially (001) GaAs wafers were used as substrates. After desorption of an oxide layer of a substrate surface, the surface was annealed at 600°C for 10 min, followed by the growth of 150-nm-thick GaAs buffer layer at 580°C . After the growth of the buffer layer, the substrate temperature was lowered to either 300°C or 250°C for the growth of a Be-doped layer. The As flux was reduced to approximately 1.0×10^{-5} Torr which is one third of the normally used As flux. The As_4 flux was used in the present MBE growth by heating the effusion cell containing a solid As. The substrate temperatures 300°C and 250°C were chosen because they were significantly lower than the normal substrate temperature for the growth of GaAs but were high enough to avoid incorporation of a high concentration of excess As [15]. The growth rate of the doped layer was varied in the range from $1.0 \mu\text{m}/\text{h}$ to $0.03 \mu\text{m}/\text{h}$ among samples by changing the Ga flux. The thickness of doped layer changed from $0.1 \mu\text{m}$ to $0.3 \mu\text{m}$.

Carrier concentrations of doped layers were estimated by the Hall effect measurement in the van der Pauw method, for which a square $5 \text{ mm} \times 5 \text{ mm}$ sample was cut and an In contact was made at each corner of the sample. Changes of lattice spacing of Be-doped epilayers from that of the substrate GaAs were determined by

rocking curve measurements of (004) reflections by using an X-ray diffractometer with a four crystal monochromator. Structure characterizations of grown layer were carried out by using transmission electron microscopy (TEM) and secondary ion mass spectroscopy (SIMS).

3. Results and discussion

Table 1 lists growth conditions, carrier concentrations and change of (004) interplaner spacing $\Delta d/d$ of 6 samples. The growth rate was changed from $1 \mu\text{m}/\text{h}$ to $0.03 \mu\text{m}/\text{h}$ which is approximately 1/30 of the normal growth rate of a GaAs layer by MBE. The Be-doped layers were grown from $0.1 \mu\text{m}$ to $0.3 \mu\text{m}$. Sample B was grown at 300°C and the lowest growth rate. The estimated hole concentration of sample B is $5.65 \times 10^{20} \text{ cm}^{-3}$. This value is significantly higher than the reported maximum concentration $2.0 \times 10^{20} \text{ cm}^{-3}$ [11] which was obtained by the MBE growth at 450°C with a normal growth rate. The Be cell temperature used for the growth of this sample was 880°C , with which a hole concentration of approximately $2 \times 10^{19} \text{ cm}^{-3}$ was obtained under the condition of the normal growth rate and a normal substrate temperature. Sample C was grown at 300°C and a normal growth rate. The Be cell temperature was set at a substantially high temperature 1030°C . The hole concentration is $3.65 \times 10^{20} \text{ cm}^{-3}$ which is approximately 2/3 of that of sample B, although $\Delta d/d$ of this sample is slightly smaller than that of sample B. Sample D was grown with the Be cell temperature 1030°C at a growth rate of $0.1 \mu\text{m}/\text{h}$. The Be

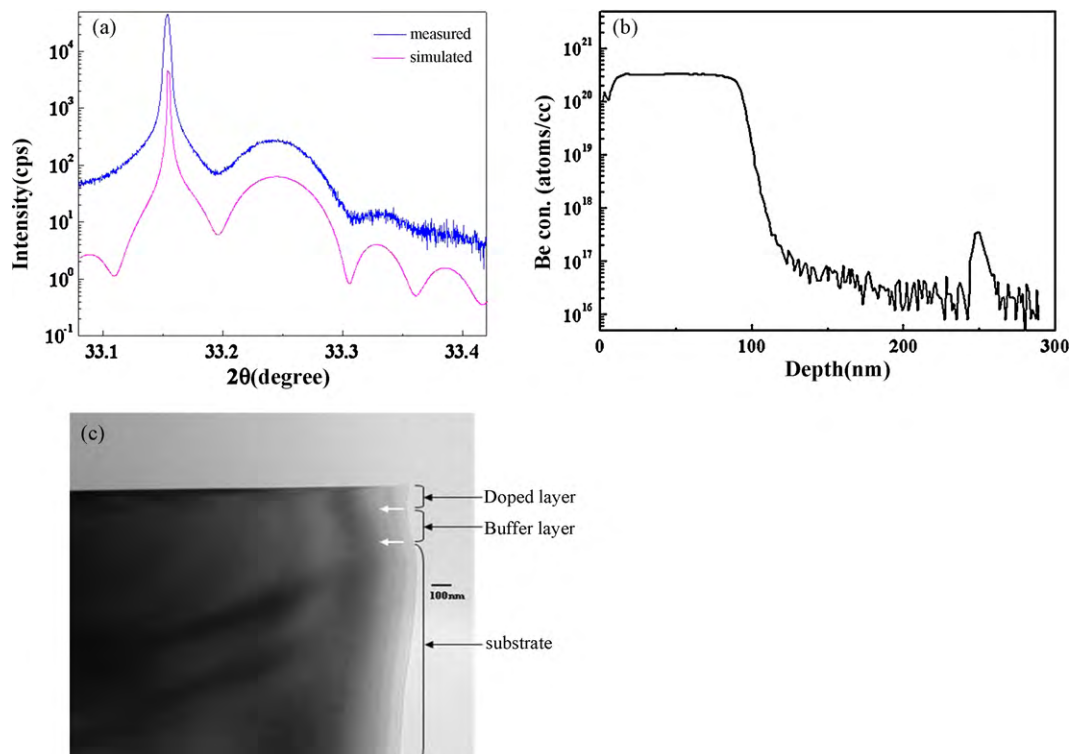


Fig. 1. (a) X-ray diffraction rocking curve, (b) SIMS profiles, and (c) cross-sectional bright field TEM image of sample B.

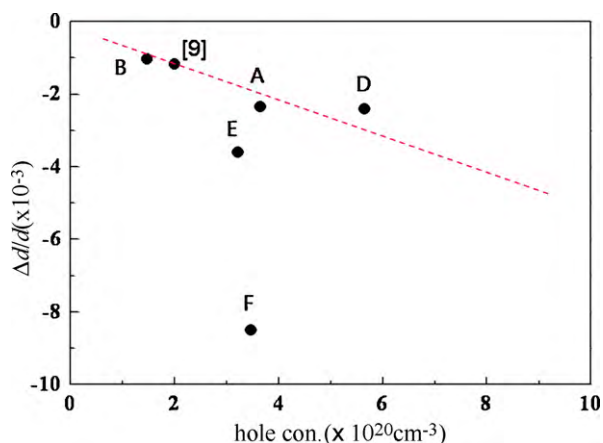


Fig. 2. Relationship between the hole concentration and the change of the lattice spacing, $\Delta d/d$ for five samples except for sample D (reference data was included in this figure).

concentration in this sample is, therefore, expected to be ten times of that of sample C. However the hole concentration and $\Delta d/d$ of sample D are considerably low as seen in Table 1. Sample E and F were grown at different growth conditions to obtain higher hole concentration, but the hole concentration although higher $\Delta d/d$ value did not increase.

Fig. 1(a), (b) and (c) are an XRD rocking curve, a SIMS profile and a bright field cross-sectional TEM image of sample B, respectively. In Fig. 1(a), we also plotted a rocking curve calculated with a model in which an interplaner spacing d_{004} is constant in the doped layer and changes abruptly into d_{004} of GaAs at the boundary with the buffer layer. Both XRD and SIMS results indicate that doped Be atoms are confined in the 0.1 μm -thick doped layer with negligible diffusion towards the buffer layer. The bright field image shows that the doped layer from the surface to the boundary with the buffer layer, which is indicated by an arrow, is defect-free in spite of a large $\Delta d/d$ value. The estimated hole concentration of sample B is substantially higher than the Be concentration indicated by the SIMS profile of Fig. 1(b). The deviation of the estimated hole concentration from the actual hole concentration, however, is considered to be a few percents at most according to the size of a square-shaped van der Pauw sample used in this measurement [16]. Because of the lack of a reliable reference sample for the SIMS measurement of a Be concentration in GaAs in the order of 10^{20} cm^{-3} , we con-

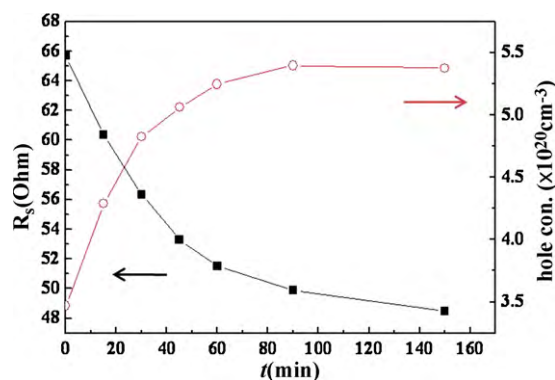


Fig. 4. Result of the sheet resistance and the hole concentration versus the annealing time, t , for sample F.

sider that the actual Be concentration in sample B is closer to the measured hole concentration than the SIMS value. A change of the (004) interplaner spacing from that of the GaAs substrate $\Delta d/d$ for sample B is also larger than twice the reported value, 1.17×10^{-3} [11], supporting the above assumption. These results of sample B, therefore, suggest that one can obtain a high hole concentration by Be-doping in the low-temperature MBE growth with a low growth rate.

Fig. 2 shows the relationship between the hole concentration and the change of the lattice spacing, $\Delta d/d$ for all samples except for sample D. As seen in Fig. 2, two regions were able to be separated. One is satisfied with the Vegard's law, which holds that a linear relation exists between the concentration and the lattice spacing. The other deviates from the Vegard's law. The hole concentration does not increase with increasing the lattice spacing. There are two possible causes for this low hole concentration. One possible cause is the existence of a high concentration of interstitial atoms. Interstitial atoms are donor that compensate holes provided by substitutional Be atoms. The effect of interstitial atoms was investigated by low-temperature annealing for sample F which was grown at 250 °C. The annealing was performed in N_2 gas flow and the annealing temperature was fixed at 300 °C. The annealing time, t , was changed from 15 min to 150 min. Fig. 3 shows the X-ray diffraction rocking curves of sample F along with changing t . The left side peak is the (004) reflection peak of the GaAs substrate and the right side peak is that of the Be-doped epilayer in Fig. 3(a). Fig. 3(b) shows only the enlarged (004) reflection peak of

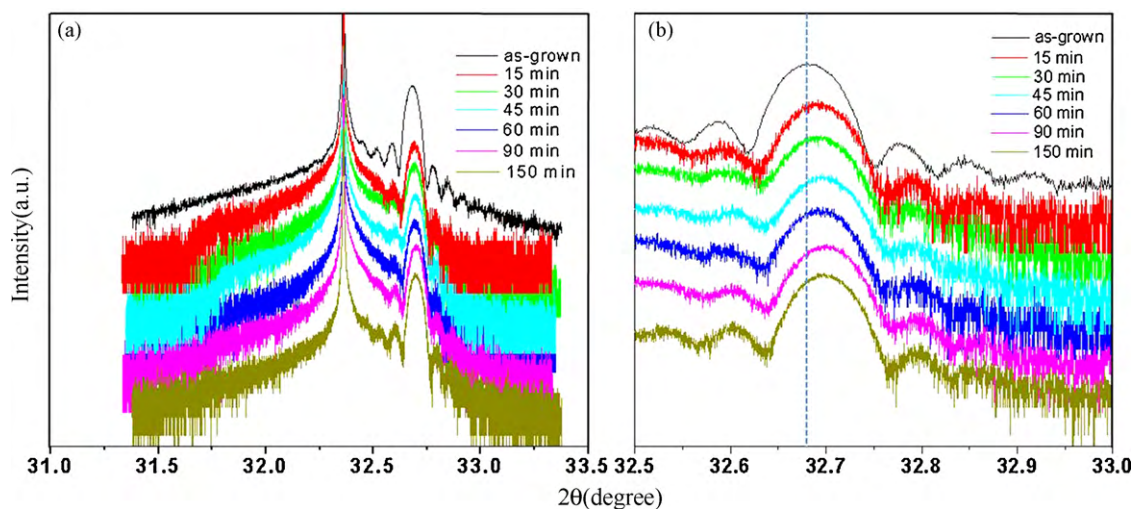


Fig. 3. X-ray diffraction rocking curves of sample F along with changing the annealing time, t .

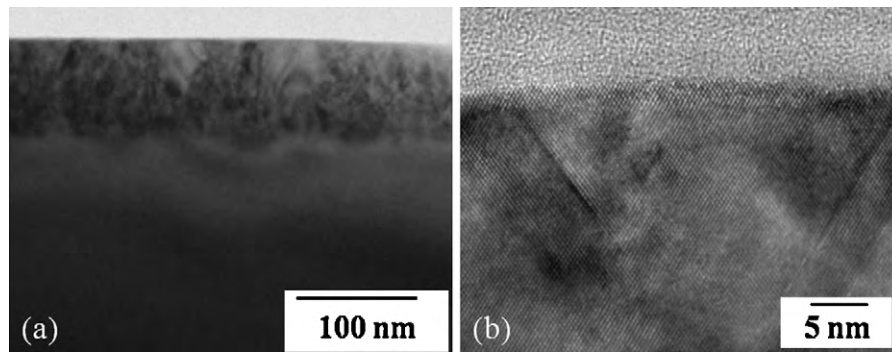


Fig. 5. (a) Cross-sectional bright field and (b) high-resolution TEM images of sample D.

the doped epilayer. As seen in figure, the peak position move the high angle side with increasing the annealing time. It is considered that the diffusion of interstitial atom such as Be interstitials, Be_i , or interstitial excess As, As_i , to the surface or the substrate occurs, then the lattice parameter of epilayer decreases.

Fig. 4 shows the result of the sheet resistance and the hole concentration versus the annealing time for sample F. The sheet resistance decreases monotonically with t while the concentration increases. The concentration, however, saturate beyond the 90 min. It can be suggested that the change of the sheet resistance is entirely due to the increase in the carrier concentration caused by the removal of compensating Be_i or As_i .

The other cause of decreasing Be concentrations with increasing the lattice spacing is the existence of defects which trap the hole. By the observation of the transmission electron microscopy the defect such as the stacking fault was found in sample D, as shown in the Fig. 5. Fig. 5(b) shows the high-resolution TEM image of same sample. The stacking fault was clearly observed. Sample D has a high density of extended defects. With a high Be cell temperature and a low growth rate, the Be concentration in this sample is expected to be significantly higher than those of other samples. It is, therefore, considered that a large lattice mismatch between the doped layer and a GaAs buffer layer led to a breakdown of the pseudomorphic growth and formation of a high density defects in this sample; these defects became sinks of the Be segregation as well as traps of free holes.

The occurrence of the defect is closely connected with the critical thickness of epilayer in the case of the heteroepitaxy. If the misfit between a bulk substrate and a growing epilayer is sufficiently

small, the first atomic layers that are deposited will be strained to match the substrate, and a coherent (or pseudomorphic) interface will be formed. However, as the epilayer thickness increases, the homogeneous strain energy becomes so large that a thickness is reached wherein it becomes favorable for misfit dislocations to be introduced. Such misfit dislocations accommodate a fraction of the misfit, so that a reduced strain remains in the over layer. It is reported that strains caused by a lattice mismatch are relaxed by introduction of partial dislocations to the interface which results in the formation of stacking faults [17]. In the present case, therefore, the existence of stacking faults suggests that partial dislocations formed in addition to perfect dislocations when the layer thickness reached the critical value.

For a single epitaxial layer, the equilibrium critical thickness, h_c , is determined by using the Matthews theory [18]. The Matthews theory predicts a critical thickness given by

$$h_c = \left(\frac{b}{8\pi\varepsilon} \right) \frac{(1 - \nu \cos^2 \alpha)}{(1 + \nu) \cos \lambda} \left[1 + \ln \left(\frac{h_c}{b} \right) \right] \quad (1)$$

where b is the Burgers vector, ε is the strain, ν is the Poisson ratio, λ is the angle between the slip direction and that direction in the film plane and α is the angle between the dislocation line and its Burgers vector.

Fig. 6 shows results of the calculation for h_c of sample E and sample F. In this calculation $\nu = 1/3$, $b = 4 \text{ \AA}$, $\cos \alpha = 1/2$, $\cos \lambda = 1/2$ are used. The value of ε is replaced by the value of the change of lattice spacing. The calculated critical thickness of sample E and F is 330 \AA and 105 \AA , respectively. However the thickness of these grown samples is thicker than the calculated h_c . These samples, therefore, have

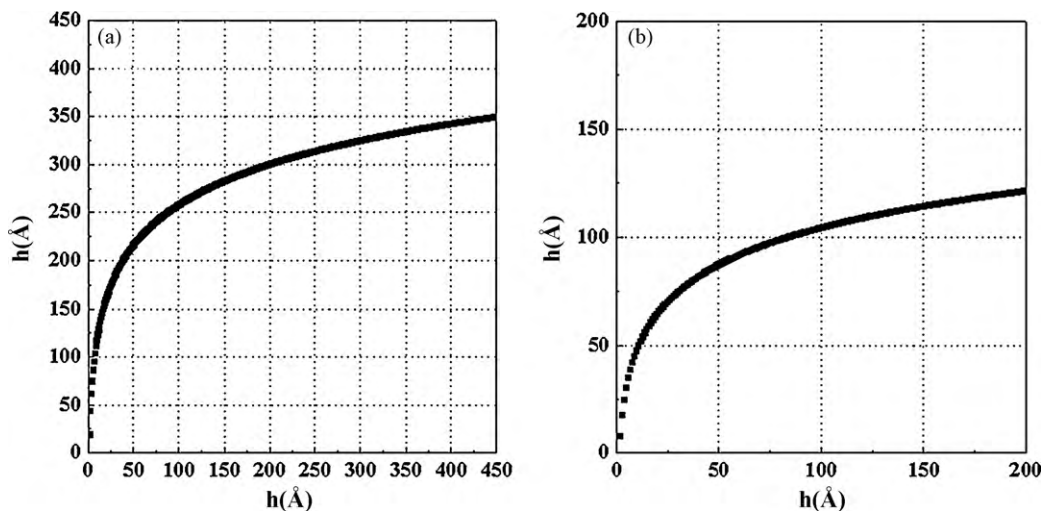


Fig. 6. Results of the calculation for critical thickness, h_c , of (a) sample E and (b) sample F, respectively.

the possibility of the occurrence of defect. So it should affect the lower concentration than that concentration which is expected by Vegard's law.

On the basis of the present results and their implications, unique properties of the low-temperature MBE growth can be described as follows. During the growth at a low temperature below 300 °C, long-distance diffusions of solute atoms such as those towards a substrate or those leading to a formation of the second phase are substantially inhibited. The Be distributions in sample B and C clearly showed this aspect. For sample B, the growth of the doped layer took 3 h due to its very low growth rate, but Be diffusions towards the buffer layer is negligible as seen in Fig. 1(a) and (b). Sample C also showed negligible diffusions towards the buffer layer, although this sample is considered to have a substantial concentration of interstitial Be atoms which are known to diffuse fast at higher temperatures.

The difference of the results of sample B and C is explained by assuming that a substitutional Be atom at a Ga site is energetically lower than an interstitial Be atom. In sample B grown at a low rate, nearly all doped Be atoms occupy substitutional sites, resulting in the low-energy configuration. In sample C grown at high rate, on the other hand, a substitutional concentration of Be atoms occupy high-energy interstitial sites due to the lack of a sufficient time for site-changes.

4. Conclusions

We have investigated the doping process of high concentrations of Be in GaAs layers by MBE at low temperatures with different growth rate in order to explore the possibility of the low-temperature MBE growth for obtaining highly non-equilibrium structures. Through the present experiments, we have obtained the following results.

The maximum hole concentration was obtained, which the sample was grown at low growth rate 0.03 $\mu\text{m}/\text{h}$ and low growth temperature 300 °C, while an increase in either the substrate temperature or the growth rate resulted in lower hole concentrations. The low hole concentration although large $\Delta d/d$ was able to be explained by the occurrence of the interstitial atoms and defects. These results suggest unique properties of the low-temperature MBE growth; long-distance diffusions of solute atoms are inhibited at a low growth temperature, while a low growth rate gives sur-

face or near-surface atoms a sufficient time to form a low-energy configuration at a low growth temperature.

The consideration of the unique properties described above is important in order to further explore the possibility of the low-temperature MBE growth. By growing a layer at a low rate one can obtain the low-energy configuration under the condition of the inhibited long-distance diffusion. The low-energy configuration, on the other hand, depends on a number of factors such as the electronic energy, strain and flux condition. Precise control of these factors, therefore, may enable one to tune a desired non-equilibrium structure such as a highly super-saturated solid solution.

Acknowledgment

This research was supported by WCU(World Class University) program and Pioneer Research Center program through the National Research Foundation of Korea funded by the Ministry of Education, Science and Technology.

References

- [1] D.C. Look, in: M.R. Brozel, G.E. Stillman (Eds.), *Properties of Gallium Arsenide*, 3rd ed., INSPEC, London, 1996, p. 684.
- [2] H. Ohno, H. Shen, A. Matsukura, F. Oiwa, A. Endo, S. Katsumoto, Y. Iye, *Appl. Phys. Lett.* 69 (1996) 363.
- [3] T. Dietle, H. Ohno, F. Matsukura, J. Cibert, D. Ferrand, *Science* 287 (2000) 1019.
- [4] K.W. Edmonds, K.Y. Wang, R.P. Campion, A.C. Neumann, N.R.S. Farley, B.L. Gallagher, C.T. Foxon, *Appl. Phys. Lett.* 81 (2002) 4991.
- [5] Ahsan M. Nazmul, S. Sugahara, M. Tanaka, *Phys. Rev. B* 67 (2003), 241308(R).
- [6] D. Chiba, Y. Nishitani, F. Matsukura, H. Ohno, *Appl. Phys. Lett.* 90 (2007) 122503.
- [7] M. Luysberg, H. Sohn, A. Prasad, P. Specht, Z. Liliental-Weber, E.R. Weber, J. Gebauer, R. Krause-Rehberg, *J. Appl. Phys.* 83 (1998) 561.
- [8] A. Suda, N. Otsuka, *Surf. Sci.* 458 (2000) 162.
- [9] E.C. Larkins, S. Harris Jr., in: R.F.C. Farrow (Ed.), *Molecular Beam Epitaxy*, Noyes Publications, Park Ridge, 1995, p. 114.
- [10] P. Enquist, G.W. Wicks, L.F. Eastman, C. Hitzman, *J. Appl. Phys.* 58 (1985) 4130.
- [11] J.L. Lievin, *Inst. Phys. Conf. Ser. No. 79*, 1986, p. 595.
- [12] W.E. Stanchina, R.A. Metzger, J.F. Jensen, D.B. Rensch, M.W. Pierce, M.J. Delaney, R.G. Wilson, T.V. Kargodorian, Y.K. Allen, *Second International Conference on Indium Phosphide and Related Materials*, No. 23–25, vol. 13, 1990.
- [13] R. Mosca, P. Bussei, S. Franchi, P. Frigeri, E. Gombia, *J. Appl. Phys.* 93 (2003) 9709.
- [14] J. Marcon, M. Ihaddadene, K. Ketata, *J. Cryst. Growth* 253 (2003) 174.
- [15] A. Suda, N. Otsuka, *Appl. Phys. Lett.* 73 (1998) 1529.
- [16] D.C. Look, *Electrical Characterization of GaAs Materials and Devices*, John Wiley, Chichester, 1989, p. 13.
- [17] W.A. Jesser, J.W. Mathews, *Philos. Mag.* 17 (1968) 461.
- [18] J.W. Matherws, A.E. Blakeslee, *J. Cryst. Growth* 27 (1974) 118.